

Experimental study of quartz classification in the enhanced gravity field using Falcon concentrator

Ling Zhang^{1,2}, Lu Yang^{1,3}, Haochun Hou¹, Yan Zhao¹, Jun Lin¹, Zeliang Zhang¹, Caiyun Bu¹, Xinran Zheng¹, Dong Fu⁴

¹ School of Resources and Environmental Engineering, Shandong University of Technology, Zibo 255000, China

² Xinjiang Engineering Technology Research Center of Biological Solid Waste Recycling, Kashi University, Kashgar 844006, China

³ Sichuan Sizhong Basalt Fiber Technology Research and Development Co., Ltd, Dazhou 635000, P. R. China

⁴ School of Chemistry and Chemical Engineering, Sichuan University of Arts and Science, Dazhou 635000, China

Corresponding author: ylpass@163.com (Lu Yang)

Abstract: The classification and separation of minerals happen in the traditional gravity separation simultaneously. This paper focuses on the classification performance of quartz particles in the enhanced gravity field. The classification efficiency of single quartz particles decreased then increased with the increase of rotational angular velocity, while it decreased with the increase of backwash water pressure. The classification efficiency of -0.5 +0.25mm, -0.25 +0.125mm, -0.125 +0.074mm, -0.074 +0.045mm and -0.045mm quartz was higher than the corresponding narrow size of -0.5mm quartz in general. The “fish-hook” phenomenon appeared in the partition curve of -0.5mm quartz under small/large rotational angular velocity and small backwash water pressure, and the dip point could be found in fine particles region, which indicated that the “fish-hook” was closely related with operating parameters and particle size. A medium rotational angular velocity and larger backwash water pressure could be helpful to avoid the appearance of “fish-hook” in fine particles region and achieve a better classification performance. This investigation is beneficial to understand the regularity of particle migration in the enhanced gravity field.

Keywords: classification, enhanced gravity field, fine particles, fish-hook

1. Introduction

Classification is a necessary unit operation for resource utilization which involving particles system (Chladek et al., 2018; Yasin et al., 2017; Rotich et al., 2015; Segets et al., 2015; Fujii et al., 2018), different products or intermediate products with different size can be treated individually and reach the maximum utilization by classification process. The main purpose of size classification was to divide a continuous wide particle size range into two or more narrow particle size ranges. Sieving, air classification and hydraulic classification are effective methods to separate minerals by size. Sieving uses the screen with fixed sieve pore to separate material accurately (Li et al., 2019; Ulusoy and Igathinathane, 2016). It is efficient and precise especially for coarse particles, while its energy consumption is nonnegligible. Air classification and hydraulic classification can be categorized as centrifugal classification which have similar principle that utilize the difference of settling velocity in the centrifugal force field (Cepuritis et al., 2015; Silventoinen et al., 2018; Tripathy et al., 2015; Laleh et al., 2017), usually used for gas-solid separation (Gu et al., 2016), gas-liquid separation (Lazrag et al., 2016), solid-liquid separation (Silva et al., 2015), and liquid-liquid separation (Motin and Bénard, 2017). Most centrifugal classification equipment, such as dust collector cyclone and hydrocyclone (Xie et al., 2018; Hwang and Chou, 2017), belong to cyclones which have advantages of simple mechanical structure, large producing capacity, easy manipulation demand and low running costs.

Enhanced gravity separator is a kind of mineral processing equipment which has similar principle with cyclone, and used for removing/reducing the gangue, impurities and harmful minerals from raw

minerals (Honaker, 1998). The centrifugal force up to 300G could reduce the lower size limit of feed and promote the separation of fine minerals (Oruç et al., 2010). The literatures showed that most researchers focused on the expansion of feed type, fluid properties, separation mechanism of particles, operating condition and operating parameters, which might be from the view of minerals separation (Oruç et al., 2010; Majumder and Barnwal, 2006; Zhu et al., 2017; Duan et al., 2009; Schriener and Anderson, 2015; Zhang et al., 2017; Kroll-Rabotin et al., 2013). However, the separation and classification of minerals particles are accompanying in the gravity separation, so the classification behaviors of minerals are inevitable and nonnegligible. Few researchers put emphasis on the classification behaviors separately in the enhanced gravity process, except that Liu had introduced the classification effect of coarse particles that above 120 μm in the froth treatment of oil sands tailings was not significant (Liu et al., 2006). The systematic and detail research on the classification performance of enhanced gravity separator is indispensable, which is helpful to interpret the lower size limit of feed, mismatch phenomenon, and the “fish-hook” phenomenon et al.

In this paper, the classification performance was investigated in enhanced gravity field using a Falcon SB40 concentrator. The quartz samples were separated at different operating parameters combination of backwash water pressure and rotational angular velocity. The classification efficiency of single size (SS) and single size in wide size range (SSIW), cut-size and separation size were used to evaluate the classification performance.

2. Materials and methods

2.1. Materials

The wide size range of -0.5mm raw quartz samples were obtained from Jiangsu province, China, which had the purity of 99.80% and density of 2.65g $\cdot\text{cm}^{-3}$. Fig. 1 represented the XRD pattern of raw quartz samples. The results showed that the sample was dominated by SiO₂ with high purity. The particle size distribution of -0.5mm raw quartz samples was shown in Fig. 2, which was measured with wet sieving method. The dominant size was -0.074 +0.045mm with percentage of 30.08%, followed by the size grain of -0.25 +0.125mm, -0.5 +0.25mm, -0.074mm and -0.125 +0.074mm. The single size quartz samples were collected from wet sieving by dividing the -0.5mm raw quartz samples into -0.5 +0.25mm, -0.25 +0.125mm, -0.125 +0.074 mm, -0.074 +0.045mm, and -0.045mm. Then the SS quartz samples were dried to prepare the SS quartz samples.

2.2. Apparatus and procedure

The classification apparatus comprises a stirred tank, peristaltic pump and Falcon SB40 concentrator as shown in Fig. 3. The quartz samples and tap water with the mass concentration of 200g/L are introduced into a stirred tank by a JJ-1 stirrer (200W) before classification tests. A peristaltic pump (TL-BT600) is employed for pumping quartz slurry to the Falcon concentrator. The Falcon concentrator (SB40) provides the enhanced gravity field using a high speed rotational bowl. The upper part of the

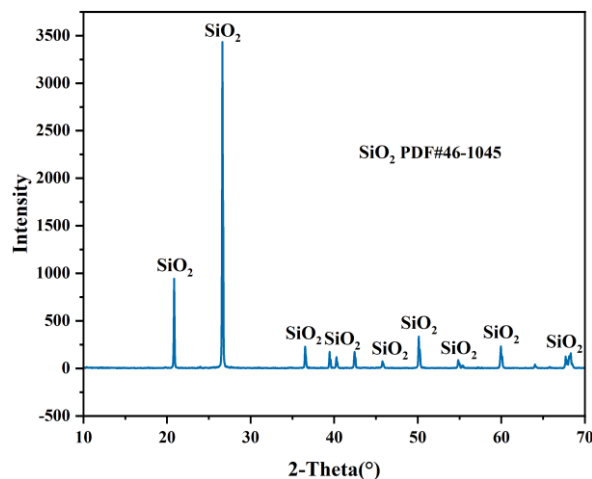


Fig. 1. XRD pattern of raw quartz

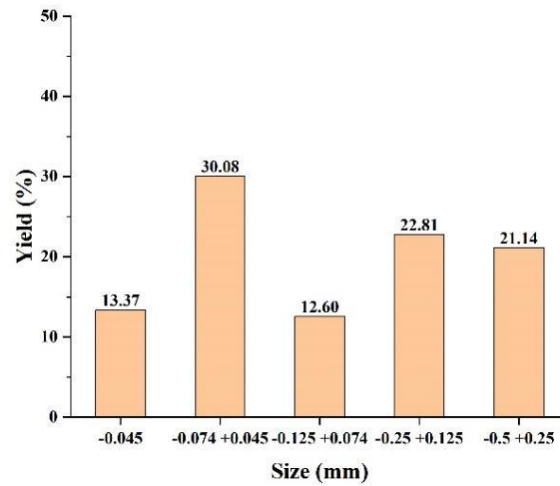


Fig. 2. Size composition of raw quartz

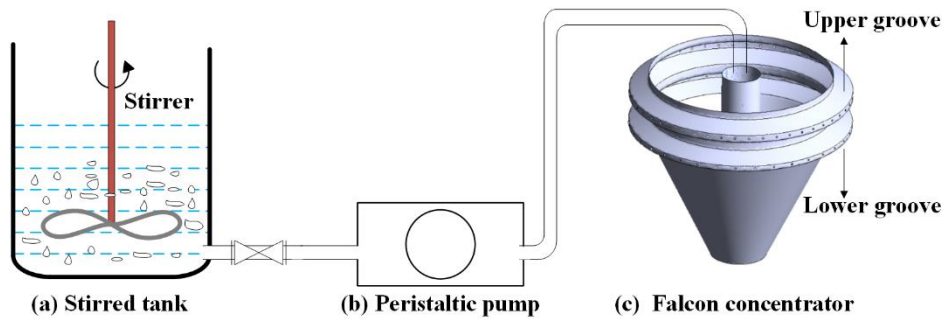


Fig. 3. Schematic of quartz classification apparatus

Table 1. Operating parameters for classification tests

Parameters	Backwash water pressure (MPa)	Rotational angular velocity (rad/s)
Value	0.01, 0.02, 0.03, 0.04, 0.05	62.83, 125.66, 188.50, 251.33, 314.16

bowl consists of two grooves with 30~50 holes in the bottom, and the lower part is an inverted cone. A maximum centrifugal force of 300G can be obtained in the high speed bowl, which drives the slurry rotating in the bowl. The feed quartz can be sorted into two products (overflow and underflow products) by Falcon concentrator at different backwash water pressure and rotational angular velocity. After the classification tests, the size distribution of underflow products and overflow products are measured using wetting sieving method. The operation parameters for classification tests are backwash water pressure and rotational angular velocity, which are listed in Table 1.

2.3. Principles of classification

The principle of particles classification and separation is the same in the enhanced gravity field. Particles classification occurs in the grooves of Falcon concentrator. A particle enter the underflow or overflow mainly depends on the resultant force acting on the particle in the radial direction. To simplify the analysis, Fig. 4 lists the three main macroscopic forces that particles experienced in the grooves, which including centrifugal force, drag force, and buoyancy force as shown in Equation (1), Equation (2), Equation (3), and Equation (4).

$$F_c = \frac{\pi d_p^3}{6} \delta \omega^2 r \quad (1)$$

$$F_b = \frac{\pi d_p^3}{6} \rho \omega^2 r \quad (2)$$

$$F'_c = \frac{\pi d_v^3}{6} (\delta - \rho) \omega^2 r \quad (3)$$

$$F_d = \psi d_v^2 v_c^2 \rho \quad (4)$$

where F_c and F_b are the centrifugal force and buoyancy force, respectively, d_v is the diameter of particle, δ and ρ are the densities of particle and fluid, ω is the angular velocity of particle, r is the radius of the bowl at which the particle is appeared. The F'_c and F_d are the effective centrifugal force of particle and drag force which acted on the particle, respectively, ψ is the drag coefficient which is closely related to the Reynolds number of fluid, v_c is the radial velocity of particle.

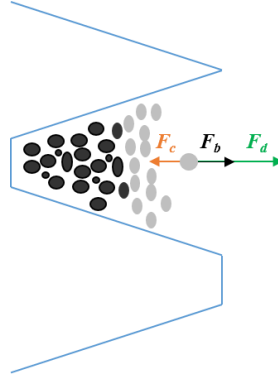


Fig. 4. Forces on a particle in the groove of Falcon concentrator

If a particles is retained in the bowl, the resultant force on the particle in the radial direction should be in the same direction as the centrifugal force, i.e. the F'_c should be at least equal to the F_d as shown in Equation (5).

$$\frac{\pi d_v^3}{6} (\delta - \rho) \frac{v^2}{r} = \frac{6\psi v_c^2 \rho}{\pi d_v \delta} \quad (5)$$

$$v_c = \sqrt{\frac{\pi d_v (\delta - \rho) \omega^2 r}{6\psi \rho}} \quad (6)$$

The Equation (6) indicates that the settling velocity of quartz particle with same density in the groove is closely related to particle size and drag coefficient. The greater the difference in particle size, the more noticeable the classification.

2.4. Estimation of classification tests

Classification efficiency (CE) is a universal index for estimating the classification performance, which represents the mass proportion of a certain size in underflow products to the feed (Kilavuz and Gülsoy, 2011). The CE is calculated by Equation (1):

$$CE = \frac{m_u}{m_f} \quad (1)$$

where m_u is the mass of a certain size in the underflow and m_f is the mass of corresponding size in the feed. The classification efficiency also can be expressed from a classification efficiency curve. Another two indexes to describe the classification performance are cut-size d_{50} and separation size d_{95} . The cut-size is defined as some particle has a possibility of 50% to enter the underflow products, and the separation size has a possibility of 95% to enter the underflow products (Kilavuz and Gülsoy, 2011; Saengchan et al., 2009; Loggenberg et al., 2016).

3. Results and discussion

3.1. The yield of single size quartz in the underflow at different operating parameters

The yield of -0.5mm, -0.5 +0.25mm, -0.25 +0.125mm, -0.125 +0.074mm, -0.074 +0.045mm and -0.045mm in the underflow was shown in Fig. 5. In the Fig. 5a, the yield of -0.5 +0.25mm in the underflow were around 100% and the quartz hardly entered the overflow at different backwash water pressure and rotational angular velocity, which indicated that the Falcon concentrator had excellent classification effect for coarse quartz. The -0.25 +0.125mm also had a high yield beyond 91% in general from Fig. 5b,

except when the rotational angular velocity was 125.66rad/s and backwash water pressure was 0.05MPa. The difference of yield in the underflow appeared with the decrease of particle. When at same rotational angular velocity of 125.66rad/s, 188.50rad/s, 251.33rad/s and 314.16rad/s, the yield of -0.125 +0.074mm, -0.074 +0.045mm and -0.045mm had a descending trend in general as the backwash water pressure ranged from 0.01MPa to 0.05MPa. And when at the same backwash water pressure, the yield first decreased then increased with the increase of rotational angular velocity. The yield of -0.125 +0.074mm were greater than 60.00%, while the yield of -0.074 +0.045mm was less than 48.60%. The finest size fraction of -0.045mm had a wide distribution from 10.18% to 100.00%. The yield of -0.5mm first decreased then increased with the increase of rotational angular velocity. These results suggested that the finer and wider particle size increased the mismatch of particles in the underflow.

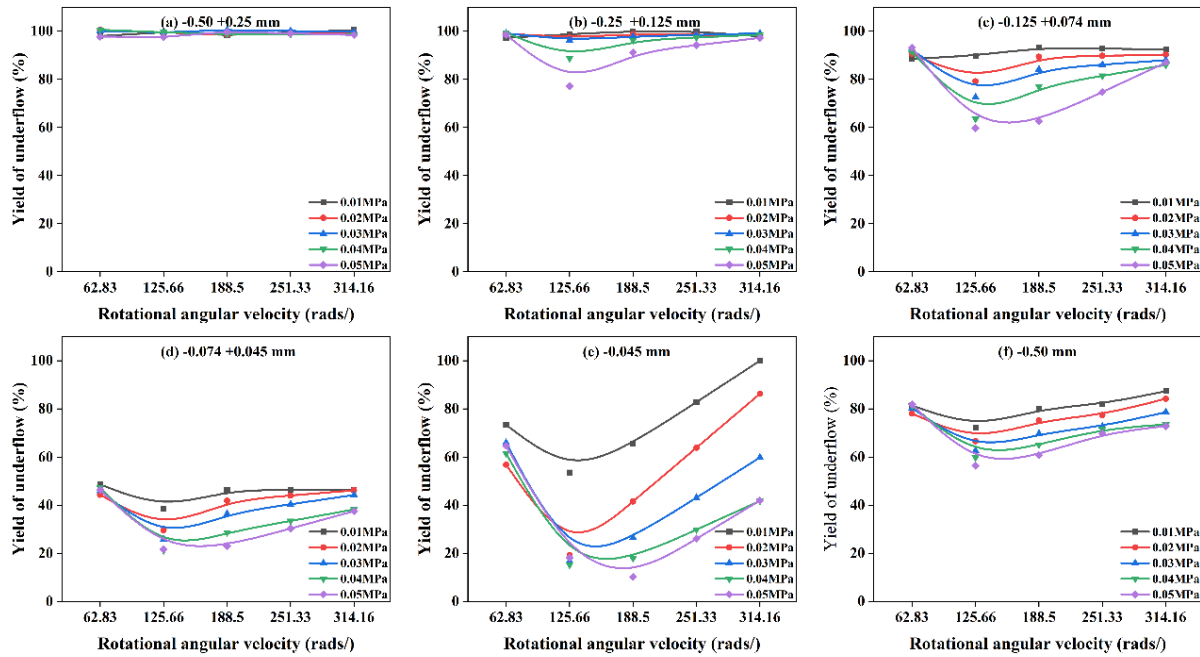


Fig. 5. The yield of each single size in underflow at different backwash water pressure and rotational angular velocity

3.2. Effect of backwash water pressure on the quartz in SS and SSIW

As can be seen from Fig. 6a, the CE of -0.5 +0.25mm in SSIW was above 97.61%, and the CE of -0.5 +0.25 mm in SS was around 100%, which indicated that the backwash water pressure had little effect on the CE of -0.5 +0.25mm quartz, and most of the -0.5 +0.25mm quartz settled in the bowl and entered the underflow products. Fig. 6b, Fig. 6c, and Fig. 6e showed that the CE of -0.25 +0.125mm, -0.125 +0.074mm and -0.045 mm in SSIW and SS decreased with the increase of backwash water pressure, and the CE of quartz in SSIW was higher than that of SS. This is due to the backwash water pressure reflecting the intensity of fluidized water injected from the holes in the grooves, and it exerts an enhanced drag force on quartz particles. The drag force experienced by the quartz particle increases with backwash water pressure for a certain rotational angular velocity. The drag force and buoyancy forces exerted on the particles can then overcome the centrifugal force, and the resultant force of quartz particles is towards the radial direction of the bowl centre, resulting in more quartz particles entering the overflow. The CE of -0.074 +0.045mm quartz in SSIW and SS decreased with backwash water pressure, and the CE in SSIW was higher than that of SS at a smaller backwash water pressure while lower than that of SS at a larger backwash water pressure from Fig. 6d. It probably due to that the -0.074 +0.045mm quartz had the largest percentage of 30.08%, which might also play the role of separation media to create a stable classification environment for other quartz particles of different size grains in the classification process.

3.3. Effect of rotational angular velocity on the quartz in SS and SSIW

As shown in Fig. 7a, The CE of -0.5 +0.25mm of SS and SSIW was close to 100% as the rotational angular

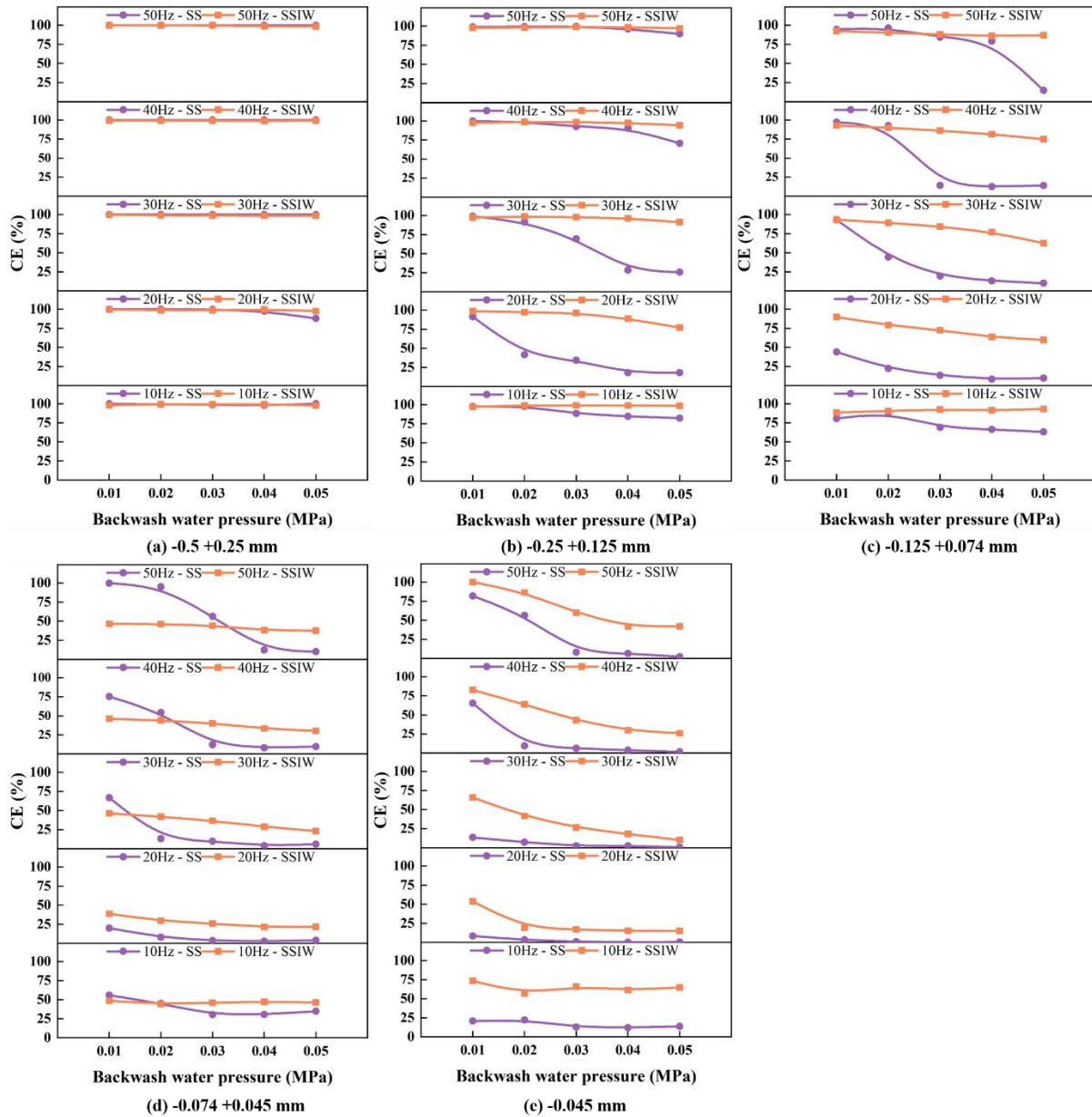


Fig. 6. The effect of backwash water pressure on the CE of quartz in SS and SSIW

velocity increased. The CE of $-0.25 + 0.125\text{mm}$, $-0.125 + 0.074\text{ mm}$, -0.045mm in SSIW was higher than that of SS and showed a trend of first increased then decreased with the increase of rotational angular velocity from Fig. 7b, Fig. 7c, and Fig. 7e. Fig. 7d presented the CE of $-0.074 + 0.045\text{mm}$ in SSIW was higher than that of SS at a lower rotational angular velocity, while lower at a higher rotational angular velocity. In general, the CE of quartz showed a trend of first decrease then increase with the increase of rotational angular velocity. The increase in rotational angular velocity means that the centrifugal force exerted on the quartz particle is increasing, and the centrifugal force tends to be greater than the drag and buoyancy forces. The resultant force on the quartz particle is towards the radial direction of the bowl wall, therefore, more quartz particles settle in the grooves and become the underflow.

3.4. The classification efficiency of -0.5mm quartz

The partition curves of -0.5mm quartz at different rotational angular velocity and backwash water pressure were demonstrated in Fig. 8~12, which illustrated the relationship of separation efficiencies versus particle size.

When the rotational angular velocity was 62.83rad/s , all the partition curves had similar “fish-hook”

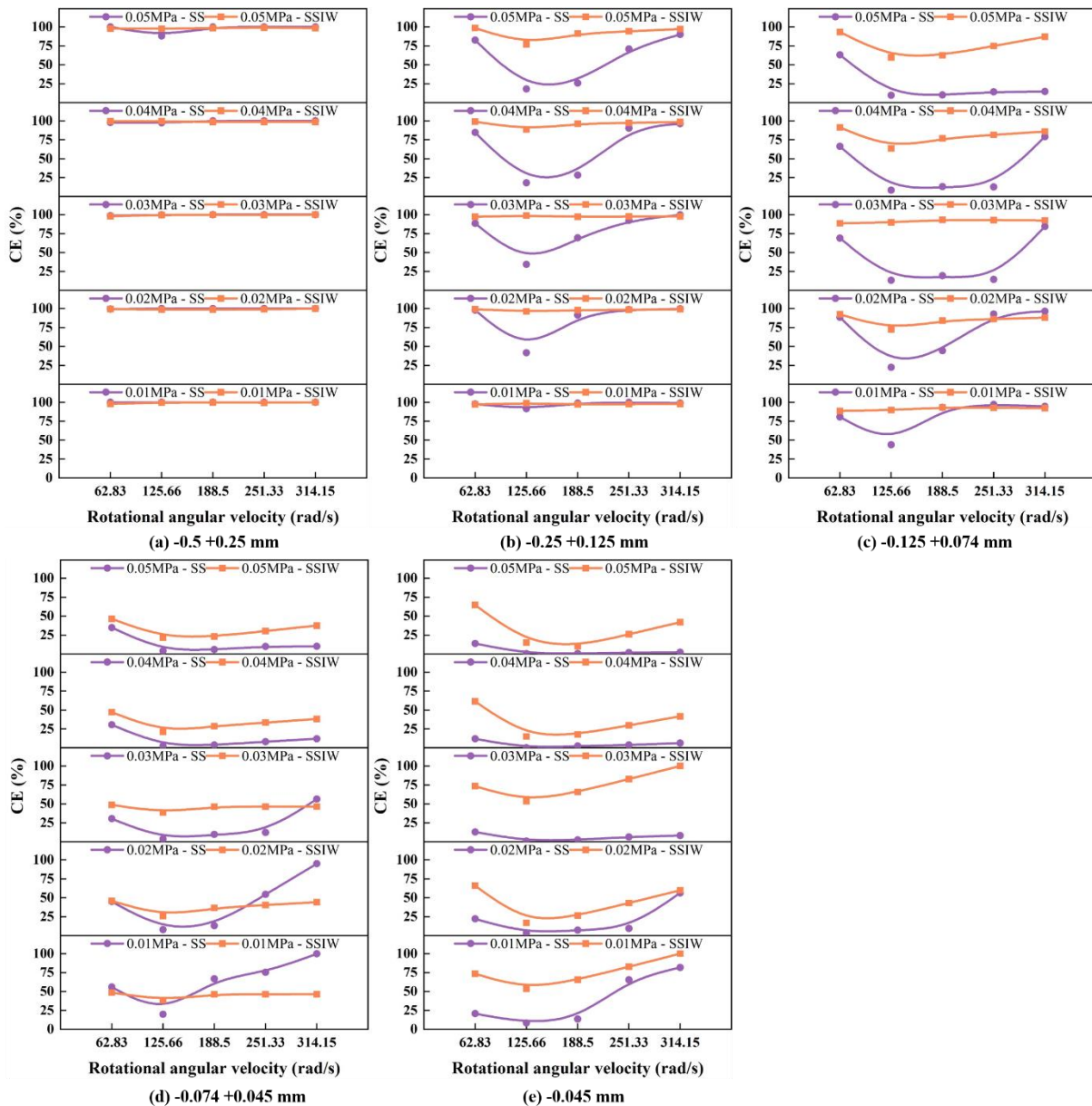


Fig. 7. The effect of rotational angular velocity on the CE of quartz in SS and SSIW

shape with backwash water varied from 0.01MPa to 0.05MPa, as shown in Fig. 8. And there were little differences among the five partition curves which suggested that the backwash water pressure had minor influences on the CE. Lv et al. (2015) introduced four regions of partition curve with “fish-hook” phenomenon from the mini-hydrocyclone classification results. These partition curves also could be divided into three regions, fish-hook region (I), separation region (II) and plateau region (III) by analyzing the characteristics of “fish-hook” shape. In the fish-hook region, the CE first decreased then increased and had typical trough with “dip point” at about 50% (Majumder et al., 2007). In the separation region, the CE had a sharp increase from 60% to 95%, which indicated that the quartz particles could be well separated in this region. The increase of CE implied the optimal size range in the classification process. The separation size d_{95} with 146.34~182.37 μm was also included in this region. In the plateau region, the quartz had a maximized CE which beyond 95%. Though the CE continued to increase slowly, it was clear that the excellent classification performance already appeared and would not improve as the size increased.

When the rotational angular velocity increased to 125.66rad/s and 188.50rad/s, the “fish-hook” phenomenon still could be found in the partition curve with backwash water pressure of 0.01MPa. The marked characteristics of CE that first decreased then increased appeared in the fish-hook region, and

the minimum of CE reached 38.53% and 46.23%, respectively. However, the partition curves with backwash water pressure from 0.02MPa to 0.05MPa presented a monotonous increase trend without “fish-hook” phenomena. The CE decreased with the backwash water pressure in general from Fig. 9 and Fig. 10, which also indicated the increase of backwash water pressure had an inhibiting effect on the classification of the same size. The cut-size d_{50} had a range of 60.57~95.04 μm and 60.26~89.81 μm , and the separation size d_{95} had a range of 46.34~182.37 μm and 145.21~282.08 μm , correspondingly.

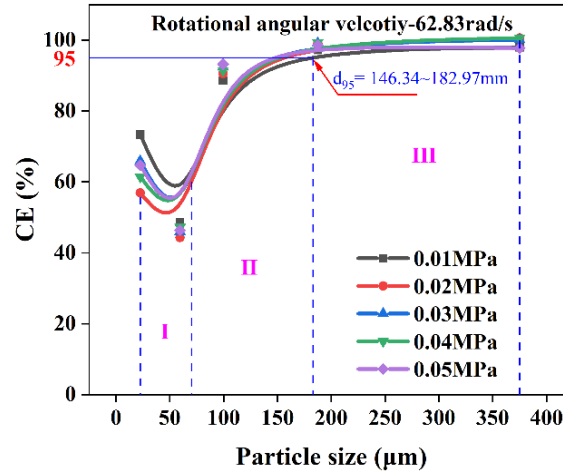


Fig. 8. Partition curves of -0.5mm quartz (rotational angular velocity of 62.83rad/s)

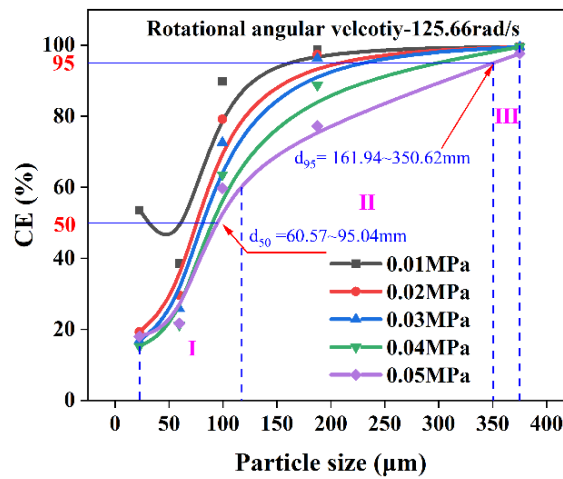


Fig. 9. Partition curves of -0.5mm quartz (rotational angular velocity of 125.66rad/s)

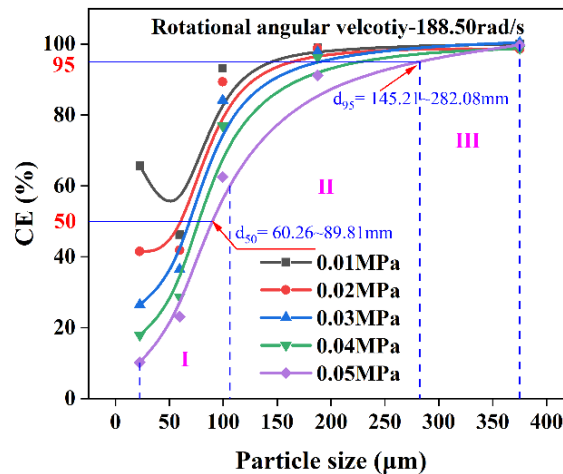


Fig. 10. Partition CE curves of -0.5mm quartz (rotational angular velocity of 188.50rad/s)

As the increase of rotational angular velocity to 251.33rad/s, the “fish-hook” phenomena were found in the partition curves with the backwash water pressure of 0.01MPa and 0.02MPa, as shown in Fig. 11, namely the “fish-hook” appeared again with the increase of rotational angular velocity. The other three curves still had similar monotonic increase trend. The cut-size d_{50} and separation size d_{95} were in the range of 62.52~76.98 μm and 142.44~252.35 μm , respectively.

When the rotational angular velocity increased to 314.16rad/s, the “fish-hook” appeared in all the five curves from Fig. 12. The partition curves were alike in shape with the rotational angular velocity of 62.83rad/s. The cut-size d_{50} in fish-hook region and separation size d_{95} in separation region were about 65.20 μm and 154.86~188.61 μm , respectively.

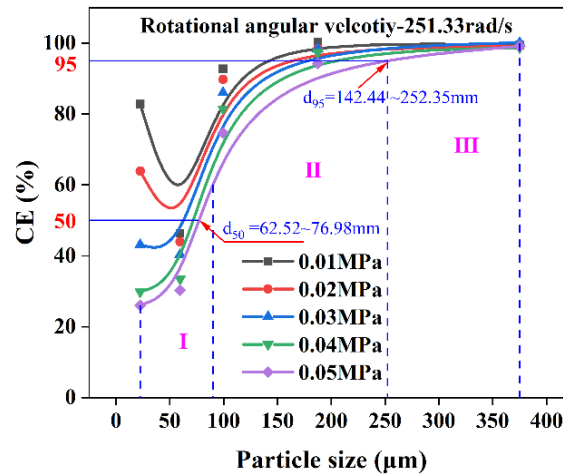


Fig. 11. Partition curves of -0.5mm quartz (rotational angular velocity of 251.33rad/s)

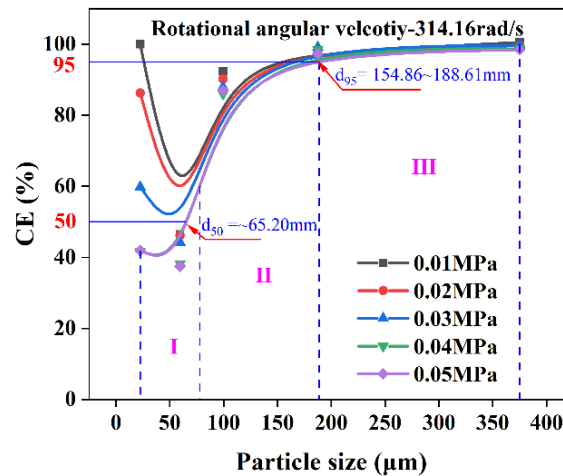


Fig. 12. Partition curves -0.5mm quartz (rotational angular velocity of 314.16rad/s)

In the range of parameters studied, the cut size of KC ranged from 60 to 100 μm , and the cut size of different types of hydrocyclones in the research of Hou et al. ranged from 60 to 130 μm as shown in Table 2, which indicated that the classification effect of KC was comparable to that of investigated hydrocyclones, and the good classification effect of KC was also worthy of attention.

3.5. Approach to avoid the “fish-hook” phenomenon

It is generally accepted that the “fish-hook” phenomenon was due to the fine mineral particles, which was also supported in chapter 3.4, and it was negative to the classification of fine minerals, therefore pre-desliming process in industry was an effective method to avoid “fish-hook” phenomenon. Meanwhile, the appearance of “fish-hook” was influenced by the operation parameters of rotational angular velocity and backwash water pressure, as presented in Fig. 13. The region of red “fish-hook” symbol appeared at smaller/larger rotational angular velocity and smaller backwash water pressure,

which indicated that medium rotational angular velocity and larger backwash water pressure could avoid the “fish-hook” phenomenon to some extent.

Table 2. The classification effects comparison of Falcon concentrator and hydrocyclones

Mineral type	Device	Size composition (Size range, yield)	Test parameters	Cut size d_{50}	Reference
Quartz	Falcon concentrator	-0.5 +0.25mm, 21.14%	62.83rad/s	-	This study
		-0.25 +0.125mm, 22.81%	125.66rad/s	60.57~95.04 μ m	
		-0.125 +0.074mm, 12.60%	188.50rad/s	60.26~89.81 μ m	
		-0.074 +0.045mm, 30.08%	251.33rad/s	62.52~76.98 μ m	
		-0.045mm, 13.37%	314.16rad/s	~65.20 μ m	
Quartz	Hydrocyclone	+0.15mm, 6.52%	CC type	62.21 μ m	Hou et al., 2022
		-0.15mm, 93.48%	CB type	95.17 μ m	
			CCC type	75.12 μ m	
			MS type	76.5 μ m	
			C type	120.68 μ m	

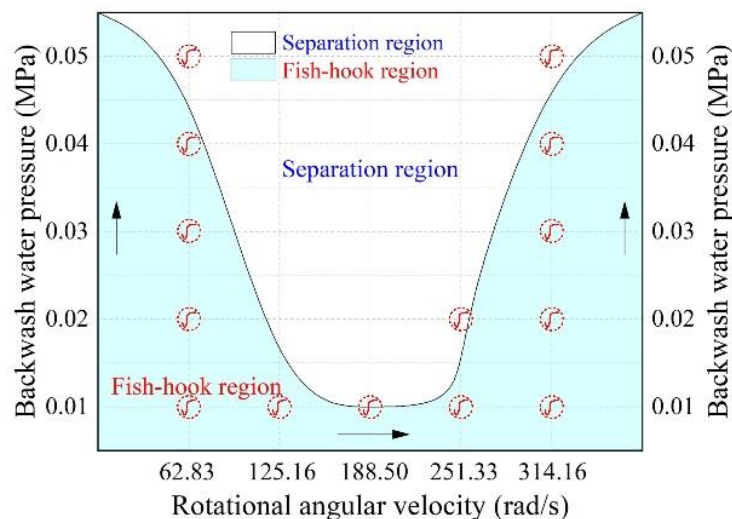


Fig. 13. Distribution of “fish-hook” under different operation parameters

4. Conclusions

The separation and classification were concomitant when processing minerals using enhanced gravity equipment. In this paper, the classification performance of quartz in the enhanced gravity field was investigated using a Falcon SB40 concentrator. The coarse quartz of -0.5 +0.074mm had preferable classification effect than the fine quartz of -0.074mm in enhanced gravity field. The classification effect was also affected by the backwash water pressure and rotational angular velocity. The CE of single size quartz particles decreased then increased with the increase of rotational angular velocity, and it decreased with the increase of backwash water pressure in general. The CE of -0.5 +0.25mm, -0.25 +0.125mm, -0.125 +0.074mm, -0.074 +0.045mm and -0.045mm quartz in SSIW was higher than in SS in general. The “fish-hook” phenomenon appeared in the partition curve under small/large rotational angular velocity and small backwash water pressure, and the dip point also could be found in the fine particle region, which showed that the “fish-hook” was closely related with the operating parameters and particle size. Therefore, lower ratio of fine particles, medium rotational angular velocity and larger backwash water pressure could be effective approach to avoid the “fish-hook” phenomenon and improve the CE of fine particles in the centrifugal classification process.

This work reveals the particle classification phenomena in the enhanced gravity field from the perspective of particle size, which is beneficial to understand the regularity of particle migration in the enhanced gravity field. Meanwhile, the good classification of narrow size particles in wide size range

particles shows its application potential to recovery valuable minerals with required size grain from waste solids. In future work, we expect to use the enhanced gravity separation technique to recover valuable elements from solid wastes, such as steel slags and bottom fly ash, while using its classification efficiency to obtain narrow fine or coarse tailings for the preparation of aggregates in building materials, in order to maximize the utilization of resources.

Acknowledgments

This work was supported by the National Nature Science Foundation of China (52004228), Natural Science Foundation of Shandong Province (ZR2021QE016), Dazhou Scientific Research Project (21ZDYF0006), and Open project of Xinjiang Engineering Technology Research Center of Biological Solid Waste Recycling (KSUGCZX202204).

References

- CEPURITIS, R., JACOBSEN, S., ONNELA, T., 2015. *Sand production with VSI crushing and air classification: Optimising fines grading for concrete production with micro-proportioning*. Miner. Eng. 78, 1-14.
- CHLAHEK, J., JAYARATHNA, C.K., MOLDESTAD, B.M., Tokheim, L.A., 2018. *Fluidized bed classification of particles of different size and density*. Chem. Eng. Sci. 177, 151-162.
- DUAN, C., WEN, X., SHI, C., ZHAO, Y., WEN, B., HE, Y., 2009. *Recovery of metals from waste printed circuit boards by a mechanical method using a water medium*. J. Hazard. Mater. 166, 478-482.
- FUJII, K., OCHI, K., OHBUCHI, A., KOIKE, Y., 2018. *Evaluation of physicochemical properties of radioactive cesium in municipal solid waste incineration fly ash by particle size classification and leaching tests*. J. Environ. Manage. 217, 157-163.
- GU, X., SONG, J., WEI, Y., 2016. *Experimental study of pressure fluctuation in a gas-solid cyclone separator*. Powder Technol. 299, 217-225.
- HONAKER, R.Q., 1998. *High capacity fine coal cleaning using an enhanced gravity concentrator*. Miner. Eng. 11, 1191-1199.
- HOU, D., ZHAO, Q., CUI, B., WEI, D., SONG, Z., FENG, Y., 2022. *Geometrical configuration of hydrocyclone for improving the separation performance*. Adv. Powder Technol. 33, 103419.
- HWANG, K.J., CHOU, S.P., 2017. *Designing vortex finder structure for improving the particle separation efficiency of a hydrocyclone*. Sep. Purif. Technol. 172, 76-84.
- KILAVUZ, F.S., GULSOY, Ö.Y., 2011. *The effect of cone ratio on the separation efficiency of small diameter hydrocyclones*. Int. J. Miner. Process. 98, 163-167.
- KROLL-RABOTIN, J.S., BOURGEOIS, F., CLIMENT, E., 2013. *Physical analysis and modeling of the Falcon concentrator for beneficiation of ultrafine particles*. Int. J. Miner. Process. 121, 39-50.
- LALEH, S., MOVAHEDIRAD, S., SARBANHA, A.A., SOBATI, M.A., 2017. *A new hydraulic particle classifier: experimental investigation and modeling*. Sep. Purif. Technol. 174, 12-21.
- LAZRAG, M., MEJIA-MENDEZ, D.L., LEMAITRE, C., STAFFORD, P.H.E., HREIZ, R., PRIVAT, R., HANNACHI, A., BARTH, D., 2016. *Thermodynamic and hydrodynamic study of a gas-liquid flow in a cyclone separator downstream supercritical drying*. J. Supercrit. Fluid. 118, 27-38.
- LI, Y., LIAO, X., LI, W., 2019. *Combined sieving and washing of multi-metal-contaminated soils using remediation equipment: A pilot-scale demonstration*. J. Clean. Prod. 212, 81-89.
- LIU, Q., CUI, Z., ETSSELL, T.H., 2006. *Pre-concentration and residual bitumen removal from Athabasca oilsands froth treatment tailings by a Falcon centrifugal concentrator*. Int. J. Miner. Process. 78, 220-230.
- LOGGENBERG, S.V., SCHOOR, G.V., UREN, K.R., VAN DER MERWE, A.F., 2016. *Hydrocyclone cut-size estimation using artificial neural networks*. IFAC-PapersOnLine 49, 996-1001.
- LV, W., HUANG, C., CHEN, J., LIU, H., WANG, H., 2015. *An experimental study of flow distribution and separation performance in a UU-type mini-hydrocyclone group*. Sep. Purif. Technol. 150, 37-43.
- MAJUMDER, A.K., BARNWAL, J.P., 2006. *Modeling of enhanced gravity concentrators—present status*. Min. Proc. Ext. Met. Rev. 27, 61-86.
- MAJUMDER, A.K., SHAH, H., SHUKLA, P., BARNWAL, J.P., 2007. *Effect of operating variables on shape of “fish-hook” curves in cyclones*. Miner. Eng. 20, 204-206.
- MOTIN, A., BENARD, A., 2017. *Design of liquid-liquid separation hydrocyclones using parabolic and hyperbolic swirl chambers for efficiency enhancement*. Chem. Eng. Res. Des. 122, 184-197.

- ORUC, F., ÖZGEN, S., SABAH, E., 2010. *An enhanced-gravity method to recover ultra-fine coal from tailings: Falcon concentrator*. Fuel 89, 2433-2437.
- ROTICH, N., TUUNILA, R., LOUHI-KULTANEN, M., 2015. *Empirical study on the effects of screen inclination and feed loading on size classification of solids by gravity*. Miner. Eng. 70, 162-169.
- SAENGCHAN, K., NOPHARATANA, A., SONGKASIRI, W., 2009. *Enhancement of tapioca starch separation with a hydrocyclone: effects of apex diameter, feed concentration, and pressure drop on tapioca starch separation with a hydrocyclone*. Chem. Eng. Process. 48, 195-202.
- SCHRINER, D., ANDERSON, C., 2015. *Centrifugal concentration of rare earth minerals from calcitic gangue*. J Metall. Eng. 4, 69-77.
- SEGETS, D., LUTZ, C., YAMAMOTO, K., KOMADA, S., SUB, S., MORI, Y., PEUKERT, W., 2015. *Classification of zinc sulfide quantum dots by size: insights into the particle surface-solvent interaction of colloids*. J. Phys. Chem. C 119, 4009-4022.
- SILVA, N.K., SILVA, D.O., VIEIRA, L.G., BARROZO, M.A., 2015. *Effects of underflow diameter and vortex finder length on the performance of a newly designed filtering hydrocyclone*. Powder Technol. 286, 305-310.
- SILVENTOINEN, P., SIPPONEN, M.H., HOLOPAINEN-MANTILA, U., POUTANEN, K., SOZER, N., 2018. *Use of air classification technology to produce protein-enriched barley ingredients*. J. Food Eng. 222, 169-177.
- TRIPATHY, S.K., BHOJA, S.K., KUMAR, C.R., SURESH, N., 2015. *A short review on hydraulic classification and its development in mineral industry*. Powder Technol. 270, 205-220.
- ULUSOY, U., IGATHINATHANE, C., 2016. *Particle size distribution modeling of milled coals by dynamic image analysis and mechanical sieving*. Fuel Process. Technol. 143, 100-109.
- XIE, B., LI, S., JIN, H., HU, S., WANG, F., ZHOU, F., 2018. *Analysis of the performance of a novel dust collector combining cyclone separator and cartridge filter*. Powder Technol. 339, 695-701.
- Yasin, Q., Du, Q., Yuan, G., Ismail, A., 2017. *Application of hydraulic flow unit in pore size classification*. SEG Technical Program Expanded Abstracts 2017. Society of Exploration Geophysicists, 3872-3876.
- ZHANG, L., TAO, Y., YANG, L., MAN, Z., 2017. *Spatial distribution of fine high-sulfur lean coal in enhanced gravity field*. Energ. Source. Part A 39, 2098-2104.
- ZHU, X., TAO, Y., SUN, Q., 2017. *Separation of flocculated ultrafine coal by enhanced gravity separator*. Particul. Sci. Technol. 35, 393-399.